Journal of Atmospheric and Solar-Terrestrial Physics 117 (2014) 95–100

Contents lists available at ScienceDirect

Journal of Atmospheric and Solar-Terrestrial Physics

journal homepage: www.elsevier.com/locate/jastp

Effects of melting layer on Ku-band signal depolarization

Thumree Sarkar, Saurabh Das, Animesh Maitra *

Institute of Radio Physics and Electronics, University of Calcutta, 92, Acharya Prafulla Chandra Road, Kolkata 700009, India

ARTICLE INFO

Article history:
Received 17 February 2014
Received in revised form
6 June 2014
Accepted 9 June 2014
Available online 18 June 2014

Keywords:
Depolarization
Ku-band
Melting layer
Rain attenuation

ABSTRACT

Propagation effects on Ku-band over an earth-space path is carried out at Kolkata, India, a tropical location, by receiving a Ku-band signal with horizontal plane polarization transmitted from the geostationary satellite NSS-6 (at 95°E). The amplitude of co-polar attenuation has been monitored along with the measurements of rain rate, rain drop size distribution and height profile of rain rate. The cross-polar enhancement of the signal is also monitored by receiving the same signal in orthogonal direction with another identical receiver. The experimental observations are used to study the effect of melting layer on both co-polar attenuation and cross-polar enhancement for the rain events observed during 2012–2013. Melting layer is indicated by the bright band signature in vertical profile of rain rate. The ground based drop size measurements indicate that the stratiform rain has more number of small drops whereas convective rain composed of large rain drops. The results indicate that the depolarization due to melting layer is more dominant compared to that due to the drop deformation mechanism at low rain rates.

1. Introduction

The recent developments in new satellite services have caused an increasing demand of bandwidth. This requires higher frequencies, such as Ku, Ka and V band for satellite communication. Rain attenuation effect on microwave propagation is severe above 10 GHz frequency which has been extensively dealt with experimental observations from temperate regions (Rastburg and Brussaard, 1993; Dintenmann et al., 1993; Bauer, 1997; Karasawa and Maekawa, 1997) as well as over tropical regions (Pan et al., 2001; Pan and Allnutt, 2004; Maitra et al., 2007, 2012; Adhikari et al., 2011; Das et al., 2010a, 2013). However, the information on the depolarization effect on these frequency bands is limited in the tropical region. The depolarization will be an important aspect of frequency re-use scheme where two orthogonal polarizations are used for communication. Again the studies on depolarization effect during rain are mostly concerned with scattering of rain drops (Ippolito, 1999) and the effect of melting layer has not been much reported.

The ice crystals in the atmosphere usually do not contribute much towards signal attenuation in the microwave range, but have a dominant effect in signal depolarization (Green, 2004). The effect of rain on signal propagation depends on rain rate as well as the rain fall type (Ippolito, 1999). The drop size distribution has an important role in causing the various propagation effects. The presence of melting layer in stratiform rain can also cause additional depolarization and attenuation of the signal. In the melting layer, ice coexists with liquid water for which the dielectric constant changes at that level. The signal polarization is affected by the presence of non-spherical particles at that level. Again, as the ice coated with liquid water also attenuates the signal, melting layer can have both depolarization as well as attenuation effect on the signal propagation (Crane, 2003; Green, 2004). Since the depth of melting layer compared to the total height of rain profile is small, the effect of melting layer in causing attenuation is much smaller compared to total rain attenuation. However, the depolarization effect of melting layer can be significant due to the non-spherical shape of ice crystals. The information of melting layer effect on satellite signal is therefore important for proper modeling of propagation effects. In this paper, the relation between rain attenuation and depolarization of Ku-band satellite signal in the presence of melting layer has been investigated with the experimental data at Kolkata (22°34′N, 88°29′E), India.

2. Experimental details

For our present study we have used the data from an impact type Disdrometer, a Micro Rain Radar (MRR) and a Ku-band signal receiving system operating at University of Calcutta, Kolkata.

* Correspondence to: S. K. Mitra Centre for Research in Space Environment, University of Calcutta, 92, Acharya Prafulla Chandra Road, Kolkata 700009, India. Tel.: +91 33 2350 9116x28; fax: +91 33 2351 5828.
E-mail addresses: thumrees1988@gmail.com (T. Sarkar), das.saurabh01@gmail.com (S. Das), animesh.maitra@gmail.com (A. Maitra).

http://dx.doi.org/10.1016/j.jastp.2014.06.006
1364-6826/

The Disdrometer (Distromet-RD-80) is used for the ground based drop size distribution and rain rate measurements. The device has a styrofoam cone to sense the momentum of rain drops. This information is then converted using the Gunn–Kinzer (Gunn and Kinzer, 1949) relation between fall velocity and drop diameter into 20 bins of rain drop sizes (from 0.3 mm to 5.5 mm) with $\pm 5\%$ accuracy (Tokay and Short, 1996). For the present study the instrument is used with an integration time of 30 s.

MRR is a vertically pointing frequency modulated continuous wave (FM-CW) radar. It transmits 50 mW power at 24.1 GHz of which a small fraction returns after getting scattered from different hydrometeors. The profile of fall velocity of the hydrometeors is estimated using the Doppler principle. Using Gunn–Kinzer relation the DSD profile is obtained from the fall velocity profile. The vertical DSD profile, in turn, gives the rain rate and radar reflectivity factor, and hence is capable of indicating the presence of melting layer by a radar bright band signature (Fabry and Zawadzki, 1995; Das et al., 2010b). The bright band represents an abrupt enhancement in vertical radar reflectivity profile due to the change in dielectric properties of melting ice (Kain et al., 2000).

The Ku-band signal at 11.172 GHz transmitted from NSS-6 geostationary satellite (at longitude 95°E) has been received at 63° elevation from our location (Maitra et al., 2007). The polarization of the Ku-band signal is horizontal with respect to the equator. At Kolkata, the local polarization angle is $-15.6°$. Both co-polar (horizontal component) attenuation and cross-polar (vertical component) enhancement have been recorded by the two receiving systems with two antennas having identical specifications. The co-polar attenuation is measured by noting the decrease in signal level, with reference to the clear air signal level, received by the horizontally polarized antenna. Again, the cross-polar enhancement is measured by noting the increase in the signal level, with reference to the clear air level, received with the vertically polarized antenna. The signal receiving system is kept under laboratory environment to make sure that the varying temperature of the surroundings does not alter the received signal amplitude.

The satellite signal is a TV broadcast signal with low fade margin of 20 dB. The separation between the co-polar attenuation and cross-polar enhancement is about 18 dB for clear air. An enhancement in the cross-polar component of the signal indicates the depolarization of the plane polarized signal caused by the propagation medium. The data are recorded with a sampling interval of 10 s. Further details of the receiving system are provided by Maitra and Chakravarty (2009).

3. Experimental results

During the month of June to September, rain mainly occurs due to South–West monsoon (June–September) in Kolkata. Rain events due to convective activities are also encountered during pre-monsoon and post-monsoon seasons. A detailed case study of rain event occurred on June 29, 2013 has been presented to indicate the rain features during monsoon of this location and its effect on the depolarization of Ku-band signal. Another example of co-polar attenuation and cross-polar enhancement for one convective and one stratiform event occurring on 19 May 2013 is also presented to support our finding. A statistical analysis of the two years data (2012–2013), pertaining to S–W monsoon is also presented. The cumulative exceedances of rainfall rates, co-polar attenuation and cross-polar enhancement are also studied for the same period. The results are also compared with ITU-R model.

3.1. Case study of the rain event on June 29, 2013

3.1.1. Rain rate and signal strength variation

The event occurring on 29 June 2013 with duration of 10 h and 30 min pertains to South–West monsoon. The maximum rain rate in the event reaches 60 mm/h, as shown in Fig. 1(a). Fig. 1 (b) shows both the co-polar attenuation and cross-polar enhancement which follow the rain rate pattern. We note that the co-polar attenuation in this event is up to 8 dB and the maximum cross-polar enhancement is 6 dB as indicated in Fig. 1(b). The anisotropy of the medium is responsible for depolarization of signal which increases with the increase in rain rate. Hence, both co-polar attenuation and cross-polar enhancement vary accordingly with the change in the rain rate.

3.1.2. Vertical profile of rain

The gradient of hydrometeor fall velocity is a good indicator to identify the melting layer as the fall velocity above melting layer is very low compared to that of melting layer region, where a sharp increase is observed. The increase in velocity is due to the phase change of ice crystals to rain drops. Melting layer is also indicated by the abrupt enhancement of radar reflectivity factor in the height profile due to melting ice crystals, called radar bright band. In case of MRR, the rain rate profile indicates the bright band much clearly than the radar reflectivity profile (Peters et al., 2005; Das et al., 2011). This is due to the fact that MRR estimates the DSD first and then the rain integral factors. The DSD measurements using MRR are valid only for melted DSD. The quantitative estimation of DSD and derived rain integral parameters in rain region are in good agreement with other ground based instruments for different regions as reported by many researchers (Peters et al., 2002,

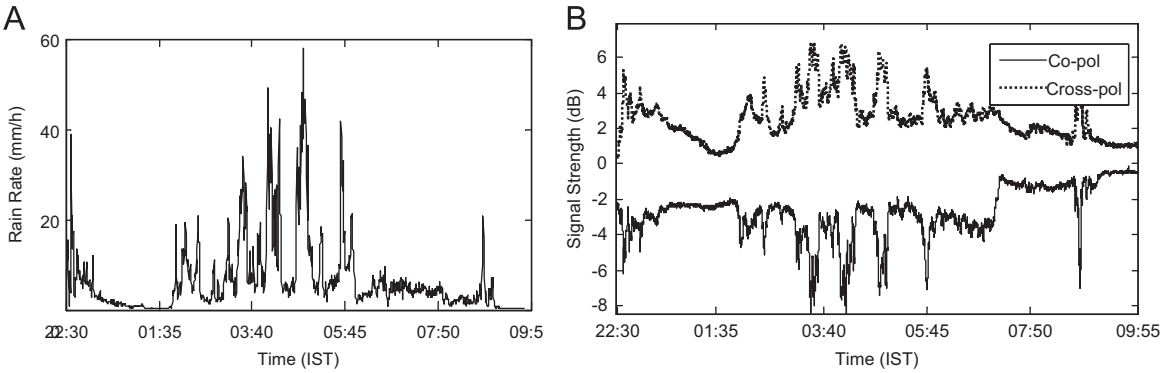

Fig. 1. Rain event recorded on 29.06.13 for (a) rain rate and (b) co-polar attenuation and cross-polar enhancement.

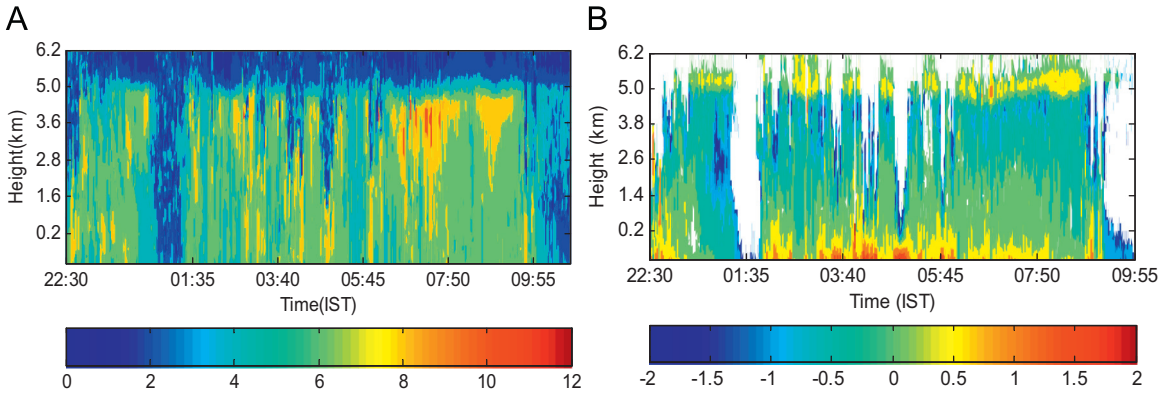

Fig. 2. Rain event recorded on 29.06.13 for (a) fall velocity profile (in m/s) and (b) rain rate height profile (in mm/h and in log 10 scale).

2005; Das et al., 2010; Kirankumar and Kunhikrishnan, 2013). The quantitative value of DSD in melting layer region is not accurate since the complex refractive index varies significantly from water to ice whereas MRR algorithm assume the presence of liquid water in all height ranges. This leads to an apparent change of the shape of the DSD. The rain rate is third moment of DSD, so the change in DSD shape around melting layer is sharply manifested in rain rate profile. Accordingly, for the present study, the fall velocity profile and rain rate profile of this event have been considered. In Fig. 2(a), which shows the fall velocity profile, we can see that above 5 km, the fall velocity is nearly zero, however, it suddenly increases to 6–8 m/s just below that height. This indicates the presence of suspended ice crystals above 5 km which falls as rain droplets with sudden increase in the velocity at the melting layer height. We can also note that the melting layer is not observed throughout total event in the fall velocity profile and indicates the presence of convective activity within stratiform rain. This is clearer in rain rate profile as shown in Fig. 2(b). From the rain rate profile we can observe significant high rain rates around 5 km which is actually due to melting layer. The intermittent presence of melting layer indicates the presence of convective activities within an event which is mostly of stratiform type.

3.1.3. Drop size distribution (DSD)

In Fig. 3(a), the ground DSD is shown for the above mentioned event. Fig. 3(a) indicates that large drops of 3–4 mm are present during this event. In Fig. 3(b), the plot between total number of drops and median volume diameter, for both convective and stratiform part of the rain, is shown. Here the median volume diameter is taken into account to study the relative dominance of rain drop sizes in stratiform and convective rain. The median volume diameter shows distinct distribution patterns of drop sizes with presence and absence of melting layer. Large median volume diameter values are observed during convective rain than during stratiform. Most of the time, the median volume diameter is below 2 mm for stratiform rain whereas the it goes up to 2.5 mm for convective rain. Similar observations are also reported by Thurai et al. (2010). This indicates that in case of stratiform rain; the number of small drops is large, compared to the convective part of rain, where large drops are abundant.

3.2. Effect of melting layer on depolarization

To assess the effect of melting layer on depolarization, we have plotted the co-polar attenuation with cross-polar enhancement of this event in Fig. 4(a). It is evident that when co-polar attenuation is below 2–3 dB, cross-polar enhancement is up to 4 dB in presence of melting layer. For high value of attenuation, cross-polar enhancement is large both with and without the presence of melting layer.

In Fig. 4(b), co-polar attenuation and cross-polar enhancement have been shown for another pair of events, one stratifom and other convective occurring on 19 May 2013. Stratiform event has rain rate lower than 10 mm/h with a clear bright band, and the convective event has maximum rain rate of 35 mm/h with no bright band. The rain structures of stratiform and convective precipitation in these events also show similar features as observed in the event occurring on 29 June 2013. For up to 3 dB attenuation, the cross-polar enhancement for stratiform rain is up to 2.5 dB but does not exceed 2 dB for convective rain. Again for attenuation value up to 3–4 dB, value of cross-polar enhancement reaches 3.5 dB when melting layer is present but does not exceed 3 dB when melting layer is not present. Attenuation values exceeding 5 dB are mostly caused by convective events having high rain rates.

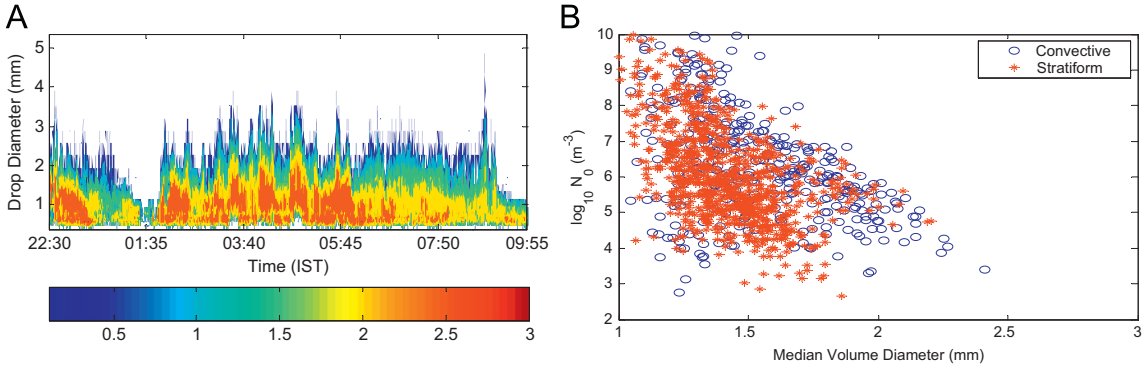

Fig. 3. (a) Drop size distribution and (b) median volume diameter vs. number concentration of rain drops for the rain event recorded on 29.06.13.

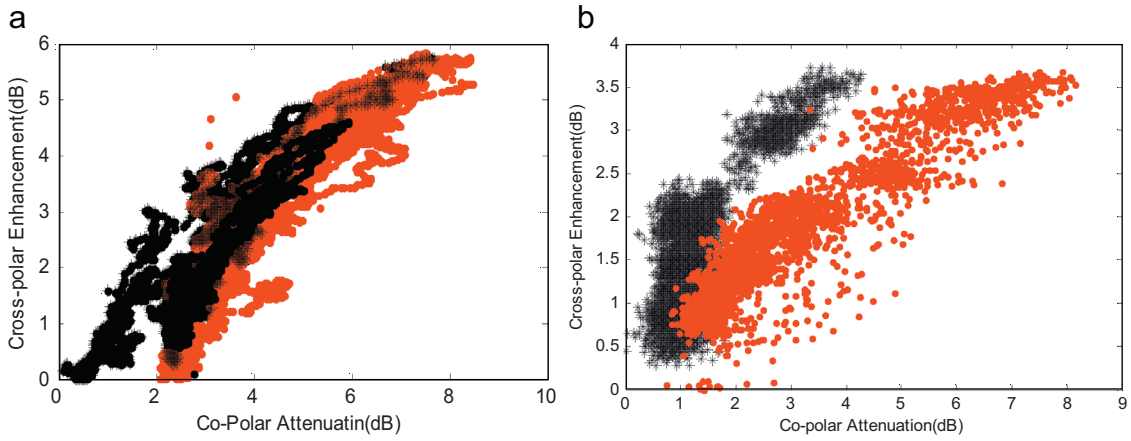

Fig. 4. (a) Co-polar attenuation (absolute value) and cross-polar enhancement observed on 29.06.13 (red dots: without bright-band, black star: with bright-band), (b) co-polar attenuation (absolute value) and cross-polar enhancement observed (red dots: convective event, black star: stratiform event). The stratiform event (having bright band) and convective event is of 19.05.13. (For interpretation of the references to color in this figure legend, the reader is referred to the web version of this article.)

3.3. Statistical analysis

For the statistical analysis, all the rain events of 2012–2013 pertaining to the S–W monsoon are considered. The rain is categorized into stratiform and convective rain by using the bright band signature from MRR fall velocity and rain rate profile. The average cross polar enhancement is then estimated for every 0.5 dB co-polar attenuation bins with its standard deviation values. The average co-polar attenuation is also estimated.

Fig. 5(a) gives the statistical results of monsoon rain data during 2012–2013. From Fig. 5(a) it can be seen that the cross-polar enhancement is always higher in presence of melting layer than for the rain without melting layer. The difference between cross-polar enhancement, with and without melting layer, for an identical value of co-polar attenuation is significant below 6 dB. The difference decreases at values higher than 6 dB of co-polar attenuation. This is because high co-polar attenuation is caused by high rain rates when large drops are prevalent, causing large depolarization, even in absence of melting layer. A major part of monsoon rain is of stratiform type, so the effect of melting layer on depolarization is prominent in addition to the effect of large oblate rain drops.

To compare our data with ITU-R model of XPD, we have used ITU-R Rec P.618-11 (2013). The XPD due to rain as per ITU-R is given as

$$\mathrm{XPD}_{\mathrm{rain}} = 26\log f + 4.1 - 12.8 f^{0.19}\log A_{\mathrm{p}} - 10\log\left[1 - 0.484(1 + \cos 4\tau)\right] - 40\log(\cos\theta) + 0.0053\sigma^2$$

where f is the frequency in GHz (11.172 GHz), A_{p} is co-polar attenuation, τ is the tilt angle with respect to local horizon ($-15.6°$), θ is the elevation angle(63°) and σ is the standard deviation of the canting angle distribution (5°).

Since in our system, we can only measure the values of co-polar attenuation and cross-polar enhancement and not the cross-polar discrimination directly, so we have calculated the XPD degradation for comparison. The XPD degradation in ITU-R model is estimated by subtracting the value of XPD at given attenuation value from clear air XPD. For our dataset the XPD degradation is calculated using the co-polar attenuation value and cross-polar enhancement as outlined by Maitra and Chakravarty (2009). The comparison has been shown in Fig. 5(b). We can observe from the figure that our result matches well with the ITU-R model for very low co-polar attenuation. But for 2–5 dB co-polar attenuation, ITU-R model overestimates our result whereas for attenuation values larger than 5 dB ITU-R model under estimates.

The exceedance probability of rain rate, co-polar attenuation and cross-polar enhancement of Ku-band signal at Kolkata are

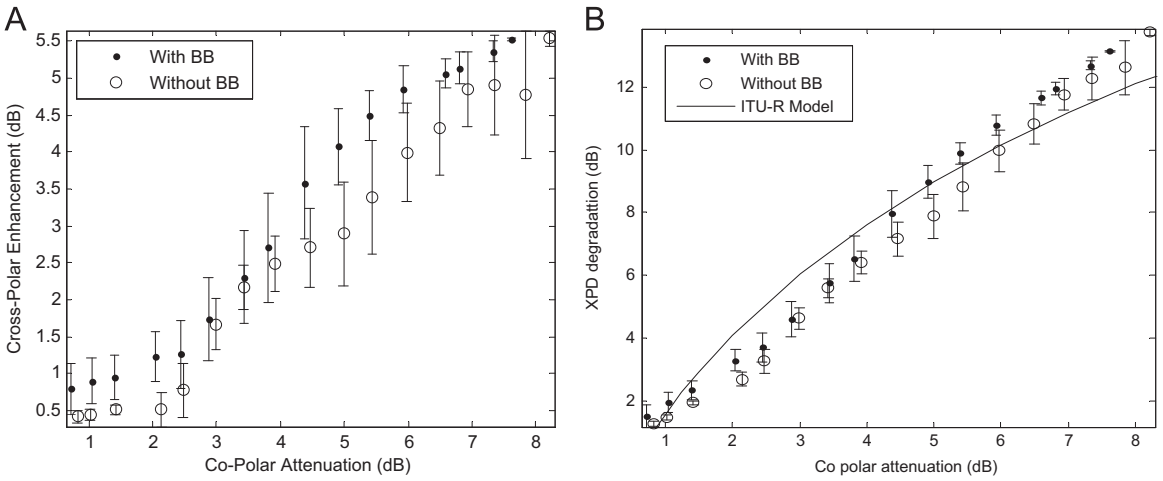

Fig. 5. (a) Mean values of co-polar attenuation and cross-polar enhancement. Vertical lines indicate the standard deviation values. (b) Comparison of ITU-R model with statistical result of XPD degradation in the presence and absence of bright band.

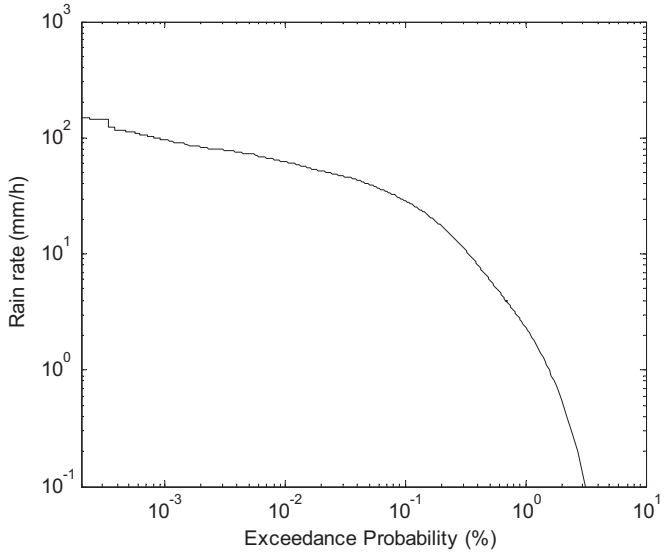

Fig. 6. Exceedence probability of rain rate.

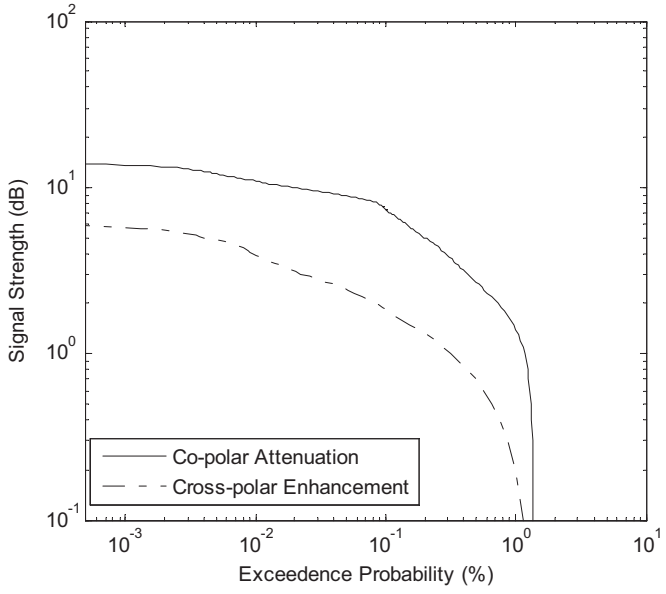

Fig. 7. Exceedence probability of signal strength.

shown in Figs. 6 and 7. It can be seen that the rain rate occurrence probability for 0.01% of time exceeds the value of 61 mm/h, which indicate high probability of rain attenuation at frequency above 10 GHz. The co-polar attenuation exceeds 10 dB for 0.01% of time and cross-polar enhancement exceeds 6 dB for the same percentage of time at Ku band frequency.

4. Conclusions

Rain attenuation and depolarization are important propagation phenomena that affect satellite communication above 10 GHz frequencies. In the present study, two years of experimental measurement of co-polar attenuation and cross polar enhancement of Ku-band satellite signal at a tropical location are utilized to investigate the interrelation between them under different raining conditions. The effect of melting layer is observed to be significant in depolarization. The statistical results indicate that the melting layer effect is more prominent in depolarizing the signal in the lower attenuation range than the higher attenuation range. At high rain rates for which large rain drops are prevalent, the rain drops are responsible for both significant cross-polar enhancement and co-polar attenuation of the signal. The XPD degradation obtained in the present study show a reasonable matching with the ITU-R model generated values. The results are important for optimum designing of the satellite communication links having orthogonal polarization in the tropical region.

Acknowledgments

Financial support provided under, (1) TEQIP Phase II, (2) ISRO sponsored “Space Science Promotion Scheme”, and (3) ISRO funded Project, “Integrated studies on water vapour, liquid water content and rain of the tropical atmosphere and their effects on radio environment”, are thankfully acknowledged.

References

Adhikari, A., Das, S., Bhattacharya, A., Maitra, A., 2011. Improving rain attenuation estimation: modeling of effective path length using Ku-band measurements at a tropical location. Prog. Electromagn. Res. 34, 173–186.
Bauer, R., 1997. Ka-band propagation measurement: an opportunity with advanced communication technology satellite (ACTS). Proc. IEEE 85, 853–862.
Crane, R.K., 2003. Propagation Handbook for Wireless Communication, System Design. CRC Press, USA; LLC.
Das, S., Maitra, A., Shukla, A.K., 2013. Diurnal variation of slant path Ka-band rain attenuation at four tropical locations in India,. Indian J. Radio Sp. Phys 42, 34–41.
Das, S., Maitra, A., Shukla, A.K., 2010a. Rain attenuation modeling in the 10–100 GHz frequency using drop size distributions for different climatic zones in tropical India. Prog. Electromag. Res. B 25, 211–224.
Das, S., Shukla, A.K., Maitra, A., 2010b. Investigation of vertical profile of rain microstructure at Ahmedabad in Indian tropical region. J. Adv. Sp. Res. 101, 78–83.
Das, S., Maitra, A., Shukla, A.K., 2011. Melting layer characteristics at different climatic conditions in the Indian region: ground based measurements and satellite observations. Atmos. Res. 101 (1), 78–83.
Dintenmann, F., Ortgies, G., Ruecker, F., Levis, R., 1993. Results from 12- to 30-GHz German propagation experiments carried out with the OLYMPUS satellite. Proc. IEEE 81, 876–884.
Fabry, F., Zawadzki, I., 1995. Long-term radar observations of the melting layer of precipitation and their interpretation. J. Atmos. Sci. 52, 838–851.
Green, H.E., 2004. Propagation impairment on Ka-band SATCOM links in tropical and equatorial regions. IEEE Trans. Antennas Propag. 46 (2), 31–45.
Gunn, R., Kinzer, G.D., 1949. The terminal velocity of fall for water droplets in stagnant air. J. Meteorol 6, 243–248.
Ippolito, L.J., 1999. Propagation Effects Handbook for Satellite System Design, 5th ed. NASA Reference Publication, USA. (Chapter 2).
Kain, J.S., Goss, S.M., Baldwin, M.E., 2000. The melting effect as a factor in precipitation-type forecasting. Weather Forecast. 15, 700–714.
Karasawa, Y., Maekawa, Y., 1997. Ka-band earth space propagation research in Japan. Proc. IEEE 85, 821–884.
Kirankumar, N.V.P., Kunhikrishnan, P.K., 2013. Evaluation of performance of Micro Rain Radar over the tropical coastal station Thumba (8.5°N, 76.9°E),. J. Atmos. Res. 134, 56–63.
Maitra, A., Chakravarty, K., Bhattacharya, S., Bagchi, S., 2007. Propagation studies at Ku-band over an earth-space path at Kolkata. Indian J. Radio Sp. Phys 36 (5), 363–368.
Maitra, A., Adhikari, A., Bhattacharya, A., 2012. Some characteristics of earth-space path propagation phenomena at a tropical location. Indian J. Radio Sp. Phys 41, 481–487.
Maitra, A., Chakravarty, K., 2009. Rain depolarization measurments on low margin Ku-band satellite signal at a tropical location. IEEE Trans. Antennas Wirel. Propag. 8, 445–448.
Pan, Q.W., Bryant, G.H., McMahon, J., Allnutt, J.E., Haidara, F., 2001. High elevation angle satellite-to-earth 12 GHz propagation measurements in the tropics. Int. J. Satell. Commun 19, 363–384.
Pan, Q.W., Allnutt, J.E., 2004. 12-GHz fade durations and intervals in the tropics. IEEE Trans. Antennas Propag. 52 (3), 693–701.
Peters, G., Fischer, B., Andersson, T., 2002. Rain observations with a vertically looking Micro Rain Radar (MRR). Boreal Environ. Res. 7, 353–362.
Peters, G., Fischer, B., Münster, H., Clemens, M., Wagner, A., 2005. Profiles of raindrop size distributions as retrieved by microrain radars. J. Appl. Meteorol 44, 1930–1949.

Rastburg, A., Brussaard, G., 1993. Propagation research in Europe using the OLYMPUS satellite. Proc. IEEE 81, 865–875.

Recommendation, ITU-R Rec P.618-11, 2013, Propagation Data and Prediction Methods Required for the Design of Earth Space Telecommunication Systems.

Thurai, M., Bringi, V.N., May, P.T., 2010. CPOL radar-derived drop size distribution statistics of stratiform and convective rain for two regimes in Darwin, Australia. J. Atmos. Ocean. Technol 27, 932–942.

Tokay, A., Short, D.A., 1996. Evidence from tropical raindrop spectra of the origin of rain from stratiform versus convective clouds. J. Appl. Meteorol 35, 355–371.